

## Supporting Information

### Facile synthesis of poly(disulfide)s through one-step oxidation polymerization for redox-responsive drug delivery

*Ruhe Zhang, ‡<sup>a</sup> Tianqi Nie, ‡<sup>b</sup> Liying Wang, <sup>c</sup> Danni He, <sup>d</sup> Yang Kang, <sup>\*e</sup> Chao Zhang <sup>\*a</sup> and Jun Wu <sup>\*f, g</sup>*

a. School of Biomedical Engineering, Shenzhen Campus of Sun Yat-sen University, Shenzhen 518107, China. E-mail: zhchao9@mail.sysu.edu.cn.

b. Guangzhou Twelfth People's Hospital, Guangzhou 510620, China.

c. Department of Hematology, The Seventh Affiliated Hospital, Sun Yat-sen University, Shenzhen, 518107, China

d. Department of Medical Ultrasonics, The Seventh Affiliated Hospital, Sun Yat-sen University, Shenzhen 518107, China.

e. Scientific Research Center, The Seventh Affiliated Hospital, Sun Yat-sen University, Shenzhen 518107, China. E-mail: kangy26@mail.sysu.edu.cn.

f. Bioscience and Biomedical Engineering Thrust, The Hong Kong University of Science and Technology (Guangzhou), Nansha, Guangzhou, 511400, China. E-mail: junwuhkust@ust.hk.

g. Division of Life Science, The Hong Kong University of Science and Technology, Hong Kong SAR, China.

‡ These authors contributed equally to this work.

\* Corresponding authors

## **Experimental Section**

### **Materials**

1,4-butanediol bis(thioglycolate) was purchased from TCI (Shanghai) Development Co., Ltd. Coumarin 6 (C6), L-glutathione (GSH, reduced form), and chloroform-*d* (CDCl<sub>3</sub>) were acquired from J&K Scientific Co., Ltd. (Beijing, China). HPLC grade solvents including dimethyl sulfoxide (DMSO), methanol, tetrahydrofuran (THF), and acetonitrile were obtained from Sigma-Aldrich. Dithiothreitol (DTT) and 1,2-distearoyl-*sn*-glycero-3-phosphoethanolamine-poly(ethylene glycol)<sub>3400</sub> (DSPE-PEG<sub>3.4K</sub>) were bought from Shanghai Yuanye Bio-Technology Co., Ltd. Docetaxel (DTX) were obtained from Huateng Pharmaceutical Co., Ltd. (Hunan, China). 4',6-diamidino-2-phenylindole (DAPI) were provided by Aladdin Industrial Corporation (Shanghai, China). Tetramethylrhodamine phalloidin (TRITC) was bought from Yeasen Biotechnology (Shanghai) Co., Ltd. DiR (1,1'-dioctadecyl-3,3,3',3'-tetramethylindotricarbocyanine iodide) was purchased from Dalian Meilun Biotech Co., Ltd. (Dalian, China).

Complete RPMI 1640 medium (Gibco) added with 1% penicillin-streptomycin and 10% fetal bovine serum was utilized to culture 4T1 cells that were bought from the American Type Culture Collection (ATCC). 4T1 cells (3–9 passages) grown to 80% confluence were used in this study. Annexin V-FITC/PI apoptosis detection kit and cell cycle assay kit were bought from KeyGEN BioTECH. Reactive oxygen species assay kits were acquired from Beyotime Biotech. Inc.

3–4 weeks female BALB/c mice were bought from the Laboratory Animal Center of Sun Yat-sen University (SYSU) and adaptively fed for one week.

### **Synthesis and characterization of the poly (disulfide)s based on 1,4-butanediol bis(thioglycolate) (PBDBM)**

Poly (disulfide)s (PBDBM) was facilely synthesized by one-step oxidation polymerization. Specifically, 5.5 mL (77.43 mmol) of dimethyl sulfoxide (DMSO) and 3 mL (15.33 mmol) of 1,4-butanediol bis(thioglycolate) (BDBM) were added into a 38 mL side branch thick wall pressure tube and mixed by stirring for 30 s. The mixture was thawed at 25 °C after freezing with liquid nitrogen and degassing the tube with a pump. This procedure was repeated three times to ensure an anhydrous and oxygen-free environment. After heating and stirring at 95 °C for 10 h, the mixture was poured into methanol to stop the reaction and placed in a 20 °C refrigerator. The precipitation was filtrated and rotated to dry. Finally, a white solid was collected with a yield of 81%. <sup>1</sup>H NMR (Bruker Avance III HD 400 MHz NMR spectrometer) and FT-IR (Thermo Scientific iN10) were used to confirm the chemical structure of the PBDBM. To investigate the redox-responsive degradation of PBDBM, 5 mg of PBDBM was dispersed in PBS (1 mL) containing 10 mM DTT at 37 °C for 12 or 24 h. After freeze-drying, the white solid was redissolved with 0.5 mL THF and filtered through a 0.22 μm membrane. The molecular weight and redox-responsive degradation of PBDBM were quantified through gel permeation chromatography (GPC) analysis, using tetrahydrofuran (THF) as the eluent.

### **Preparation and characterization of PBDBM-based nanoparticles**

The nanoprecipitation method was used to prepare both blank PBDBM nanoparticles (PBDBM NPs) and DTX-loaded nanoparticles (DTX@PBDBM NPs). Specifically, stock solutions of PBDBM, DSPE-PEG<sub>3,4K</sub>, and DTX in DMSO with a concentration of 20 mg mL<sup>-1</sup>, 10 mg mL<sup>-1</sup>, and 10 mg mL<sup>-1</sup> were prepared, respectively. After screening the DTX content, stock solutions were mixed with the optimal volume ratio (PBDBM: DSPE-PEG<sub>3,4K</sub>: DTX: DMSO=10: 4: 3: 3). For blank PBDBM NPs, DTX was replaced by an equal volume of DMSO. Then, 100 μL mixed stock solution (oil phase) was dropwise added into 1 mL ultrapure water at an optimal oil: water ratio of 1: 10 under magnetic stirring. The above NPs solution was concentrated and purified

twice with ultrapure water to remove free DTX and organic solvent with an ultrafiltration tube (MWCO 100 kDa). For further use, physiological NPs solution was acquired by adding nine parts of the concentrated NPs solution with one part of 10× PBS.

Their particle sizes and zeta potentials were determined using a Zetasizer Nano ZS90 instrument (Malvern Instruments Ltd, UK). The morphology of PBDBM NPs and DTX@PBDBM NPs were acquired and imaged with a transmission electron microscope (TEM, JEOL, JEM-2010). The stability of both NPs in PBS was characterized by dynamic light scattering (DLS) for 7 days to measure the changes in particle size and polydispersity index (PDI). The loading capacity (LC) and loading efficiency (LE) of DTX@PBDBM NPs were measured by high-performance liquid chromatography (HPLC). The DTX@PBDBM NPs solution was added with the same volume of acetonitrile and treated with ultrasound for one hour to destroy the nanoparticles and release the encapsulated drugs. Then supernatant after centrifugation was filtered using a 0.22 μm filter and transferred into a liquid injection vial. The DTX content was analyzed by an Agilent 1260 Infinity II apparatus equipped with an Agilent ZORBAX Eclipse XDB-C18 column (4.6 mm × 150 mm, 5 μm). The mobile phase was a 65: 35 (v/v) mixture of acetonitrile and water pumped at a flow rate of 1 mL min<sup>-1</sup>. The calibration curve for DTX was constructed with the ultraviolet absorption at 230 nm. The LC and LE were calculated according to the following formulas:

$$LC (wt\%) = \frac{\text{Mass of loaded DTX}}{\text{Mass of DTX@PBDBM NPs}} \times 100 \quad (1)$$

$$LE (wt\%) = \frac{\text{Mass of loaded DTX}}{\text{The total mass of feeding DTX}} \times 100 \quad (2)$$

To analyze the ability of DTX@PBDBM NPs to release DTX within the reductive microenvironment of tumor cells, DTX@PBDBM NPs were added to 10 mM GSH. The size of DTX@PBDBM NPs was measured with a Zetasizer Nano ZS90 instrument at 0, 10 min, 30 min, 1 h, 2 h, 3 h, and 4 h.

### **Redox-responsive drug release behavior of DTX@PBDBM NPs**

The redox-responsive DTX release behavior of DTX@PBDBM NPs was studied using the dialysis method. In detail, a solution of DTX@PBDBM NPs was aliquoted (1 mL) and transferred into several dialysis bags (molecular weight cut-off = 3500 Da), which were then placed in a 15 mL centrifuge tube containing 10 mL PBS including 1% polysorbate 80 (v/v) as the prescribed release medium (GSH concentration: 0, 2  $\mu$ M, 10 mM). The centrifuge tubes were kept in an oscillator that maintained a constant temperature of 37 °C and a continuous shaking speed of 100 rpm. At specific time points, 200  $\mu$ L of the outside release medium was withdrawn followed by replacing it with an equal volume of fresh release medium. The DTX content of the above-collected medium was determined by HPLC according to the method described above and the cumulative release rate was calculated.

### **Cellular uptake evaluation**

To visualize the cell uptake and cell distribution of PBDBM NPs, PBDBM NPs loaded with C6 (C6@PBDBM NPs) were prepared by replacing DTX with C6 and observed by Confocal laser scanning microscopy (CLSM, ZEISS880, Germany). Flow cytometry (CytoFLEX S, Beckman Coulter, United States) was also utilized to quantify cell uptake. For the CLSM cell uptake experiment, 4T1 cells ( $1 \times 10^5$  cells) were counted, seeded onto a 15 mm glass confocal dish with 1 mL 1640 medium, and grown for 12 h. Thereafter, the medium was superseded with fresh medium containing C6@PBDBM NPs or free C6 with an equivalent C6 concentration of 1  $\mu$ g mL<sup>-1</sup> and incubated for 10 min, 1 h, 3 h, or 6 h separately. After washing with PBS twice, 4T1 cells were sequentially fixed with paraformaldehyde (4%, Beijing Labgic Technology Co., Ltd) for 15 min, permeabilized with Triton X-100 solution (0.5%) for 5 min, stained with tetramethylrhodamine (TRITC) phalloidin at 37 °C for 15 min, and with DAPI (1  $\mu$ g mL<sup>-1</sup>) for 5 min. Between the above steps, 4T1 cells were rinsed three times with 1 mL PBS and finally stored in PBS. A 60 $\times$  objective lens was utilized for CLSM imaging.

For the flow cytometry assay, 4T1 cells ( $2 \times 10^5$ /well) were placed onto a 6-well plate and grown for 12 h. After treatment with C6@PBDBM NPs for 10 min, 1 h, 3 h, or 6 h respectively, the 4T1 cells were trypsinized and rinsed with PBS three times before flow cytometric quantitative analysis.

### **In vitro cytotoxicity of DTX@PBDBM NPs**

In vitro cytotoxicity of DTX, blank PBDBM NPs, and DTX@PBDBM NPs were evaluated by the MTT assay. 4T1 cells (3000 cells per well) were seeded in 96-well microplates. After culturing for 24 h, the medium was swapped with 200  $\mu$ L of medium supplemented with free DTX, PBDBM NPs, or DTX@PBDBM NPs at different concentrations. After incubation for 48 h, each well was appended with 20  $\mu$ L of the MTT solution (5 mg mL<sup>-1</sup>). After another 4 h incubation to form formazan crystals from living cells' mitochondria, all medium was carefully aspirated and replaced with 150  $\mu$ L of DMSO. The microplate was gently shaken for 5 min and read by a microplate reader (490 nm, BioTek). Cell viability was reckoned according to the relative absorbance as follows:

$$\text{cell viability (\%)} = \frac{OD_{\text{sample}} - OD_{\text{blank}}}{OD_{\text{control}} - OD_{\text{blank}}} \times 100 \quad (3)$$

### **In vitro cell apoptosis evaluation**

In vitro cell apoptosis was detected by an Annexin V-FITC/PI assay. 4T1 cells (200,000 cells/well) were placed and incubated in 6-well plates for 24 h. After replacing the medium, the 4T1 cells were maintained with medium (2 mL) supplemented with DTX, blank PBDBM NPs, and DTX@PBDBM NPs (equivalent DTX concentration: 0.25  $\mu$ g mL<sup>-1</sup>) for 48 h. Subsequently, cells were collected after digestion with trypsin (0.25%, EDTA free, 1 $\times$ ) and rinsed twice with PBS. Then, the 4T1 cells were stained with Annexin V-FITC and propidium iodide (PI) according to the protocol of the apoptosis kit and analyzed via flow cytometry for quantitative apoptosis.

### **Cell cycle measurement**

The pre-treatment of the cell cycle experiment was like the apoptosis experiment, except that the treatment time was changed from 48 h to 24 h. Then, 4T1 cells were digested with trypsin-EDTA (0.25%, 1×) and washed with PBS before fixing with 70% ethanol for 12 h at 4 °C. After centrifuging to remove the ethanol and washing with PBS. Then, the 4T1 cells were incubated with Rnase A and PI for 30 min at room temperature and further analyzed via flow cytometry.

### **Intracellular ROS detection**

Intracellular ROS detection was detected with 2',7'-dichlorofluorescein diacetate (DCFH-DA) as a probe for flow cytometry. 4T1 cells (200,000 cells/well) were placed and incubated in 6-well plates for 12 h. Then, the 4T1 cells were cultivated with medium (2 mL) containing free DTX, blank PBDBM NPs, and DTX@PBDBM NPs (equivalent DTX concentration: 0.5 µg mL<sup>-1</sup>) for 12 h, respectively. Next, the cells were harvested with trypsin and incubated with serum-free 1640 medium supplemented with DCFH-DA with a concentration of 10 µM for 30 min at 37 °C. After washing with PBS three times to completely remove excess DCFH-DA, the cells were finally resuspended in 0.5 mL PBS and detected with flow cytometry in the FITC channel.

### **Hemolytic analysis**

To enable safe intravenous injection of NPs, blood compatibility of PBDBM NPs and DTX@PBDBM NPs was first examined by a hemolysis test. The red blood cells (RBCs) isolated from anticoagulant BALB/c mouse blood were resuspended to a 4% stock suspension after washing with an isotonic physiological buffer five times. Negative control (1 × PBS), positive control (water), or different concentrations of PBDBM NPs and DTX@PBDBM NPs were mixed with the RBCs suspension with equal volume in 1.5 mL tubes, respectively. All tubes were shaken at a speed of 100

rpm at 37 °C for 3 h following centrifugation for 5 min (1000 rpm). The supernatant was transferred to a 96 plate and read by a microplate reader at 540 nm. The hemolysis percentage was calculated according to the equation below:

$$\text{Hemolysis rate (\%)} = \frac{OD_{\text{sample}} - OD_{\text{negative}}}{OD_{\text{positive}} - OD_{\text{negative}}} \times 100 \quad (4)$$

### **In vivo biodistribution study**

The in vivo biodistribution of PBDBM NPs loaded with DiR (DiR@PBDBM NPs) was evaluated utilizing the 4T1 orthotopic tumor model, which was developed by orthotopically implanted 4T1 cells ( $1 \times 10^6$ ) in the right mammary fat pad of BALB/c mice. The mice were randomly grouped into free DiR and DiR@PBDBM NPs (intravenously DiR dose:  $0.2 \text{ mg kg}^{-1}$ ) once the tumor size grew to over  $500 \text{ mm}^3$ . All mice were anesthetized, and the NIR signals were collected with an IVIS Spectrum In Vivo Imaging System (PerkinElmer, United States) at scheduled time points. Following 24 h of injection, mice were randomly selected from each group and sacrificed. The main tissues (heart, lung, liver, spleen, and kidney) and tumors were withdrawn, washed with PBS, and imaged. All the acquired images were analyzed using Live Imaging®4.4 Software.

### **Antitumor efficacy study**

4T1 orthotopic tumor model was developed as mentioned above. Once the tumor size grew to just about  $100 \text{ mm}^3$ , the mice were randomly grouped ( $n = 5$ ) into PBS (control group), PBDBM NPs, free DTX, and DTX@PBDBM NPs at an equivalent DTX dose of  $5 \text{ mg kg}^{-1}$ . The formulas were administered by intravenous injection every three days five times. The first administration time was set as day 0. The body weight, tumor length (a), and width (b) were measured from day 0 every alternate day. The volume of the tumor (V) was calculated as  $V = 0.5 \times a \times b^2$ . All mice were sacrificed after 16 days of the first administration. The blood, major tissues, and tumors were sampled. Serums



obtained by centrifugation after blood standing for 30 min were used for biochemical analysis, including alkaline phosphatase (ALP), alanine transaminase (ALT), aspartate transaminase (AST), blood urea nitrogen (BUN), and creatinine (CREA). After fixation in a 4% paraformaldehyde solution, hematoxylin and eosin (H&E) staining was applied for tumors and major tissue sections. Terminal deoxynucleotidyl transferase-mediated dUTP nick-end labeling (TUNEL) staining was also performed on tumor sections to assess the tumor apoptosis of each group.

### **Statistical analysis**

The statistical analysis of data was conducted using SPSS software. One-way analysis of variance (ANOVA) was applied to analyze multiple groups. Significant difference was shown as \* $p < 0.05$ , \*\* $p < 0.01$  or \*\*\* $p < 0.001$ . # on the top of the bar is compared to the control or PBS group.

**Table S1** Screening of DTX@PBDBM NPs with different oil:water ratio and DTX content

<b>Oil:water ratio-DTX Content (wt% )</b>	<b>Size <math>\pm</math> SD (nm)</b>	<b>PDI <math>\pm</math> SD</b>	<b>Zeta potential <math>\pm</math> SD (mV)</b>	<b>LC (%)</b>	<b>LE (%)</b>
1:5-5%	166 $\pm$ 5.1	0.126 $\pm$ 0.032	-45.2 $\pm$ 1.6	1.11	23.40
1:10-5%	172 $\pm$ 0.5	0.089 $\pm$ 0.069	-25.6 $\pm$ 2.4	2.03	42.63
1:20-5%	180 $\pm$ 2.4	0.066 $\pm$ 0.050	-27.8 $\pm$ 1.7	1.12	23.61
1:5-10%	169 $\pm$ 0.5	0.103 $\pm$ 0.071	-24.3 $\pm$ 3.1	1.92	21.07
1:10-10%	154 $\pm$ 1.4	0.149 $\pm$ 0.031	-20.0 $\pm$ 2.1	3.60	39.60
1:20-10%	185 $\pm$ 7.8	0.078 $\pm$ 0.095	-28.1 $\pm$ 3.3	3.51	38.63
1:5-15%	177 $\pm$ 7.3	0.041 $\pm$ 0.030	-24.2 $\pm$ 4.3	4.14	31.77
1:10-15%	143 $\pm$ 2.3	0.153 $\pm$ 0.041	-28.6 $\pm$ 0.3	6.13	46.99
1:20-15%	179 $\pm$ 5.6	0.153 $\pm$ 0.038	-26.1 $\pm$ 1.5	5.15	39.52

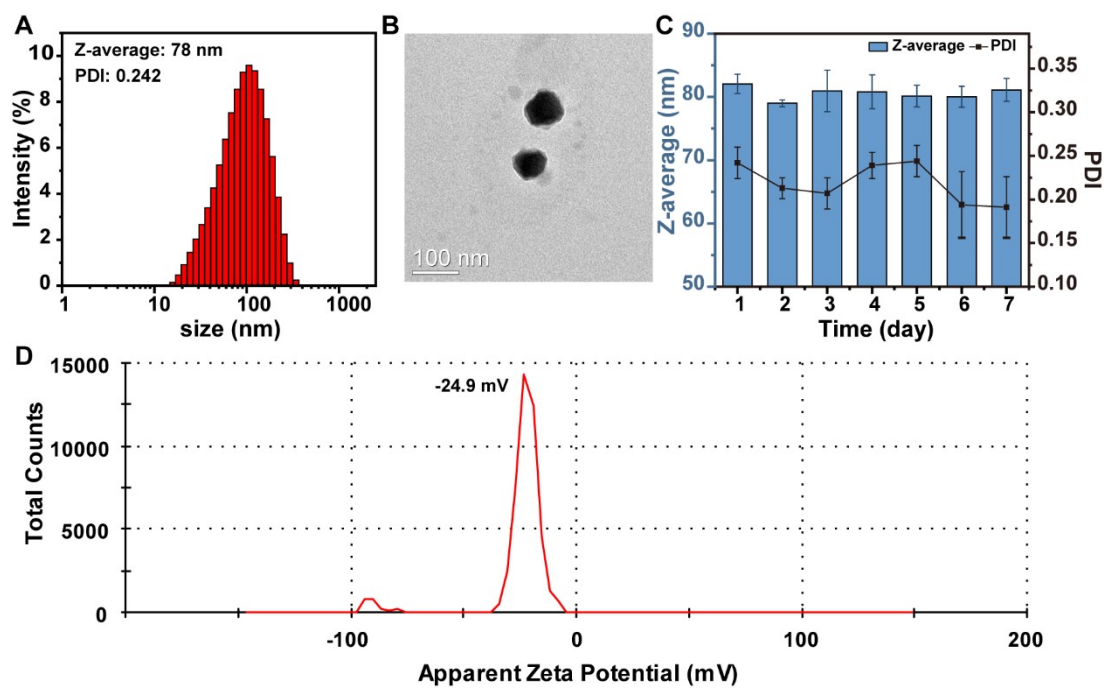


**Fig. S1.** Characterization of PBDBM NPs. (A) Size distribution of PBDBM NPs. (B) TEM image of PBDBM NPs. (C) Stability of PBDBM NPs. (D) Zeta potential of PBDBM NPs.

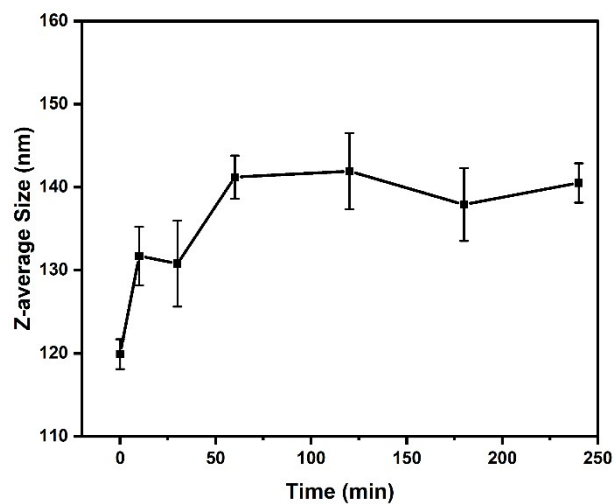


**Fig. S2.** Z-average size variation of DTX@PBDBM NPs in 10 mM GSH for different times.

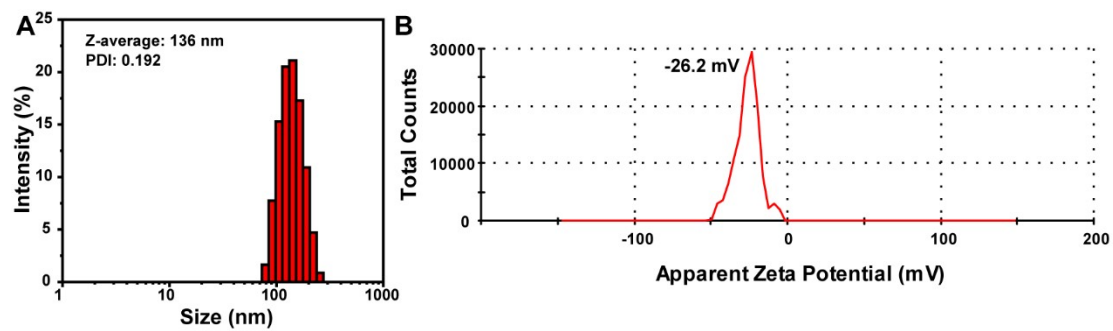


**Fig. S3.** Characterization of C6@PBDBM NPs. (A) Size distribution of C6@PBDBM NPs. (B) Zeta potential of C6@PBDBM NPs.

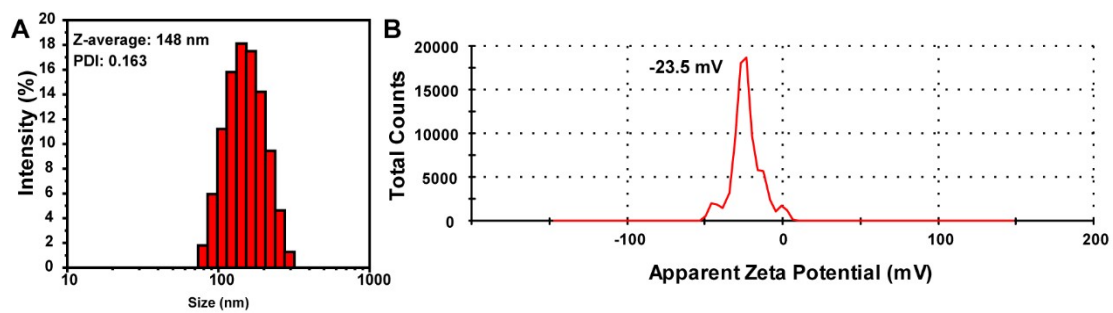


**Fig. S4.** Characterization of DiR@PBDBM NPs. (A) Size distribution of DiR@PBDBM NPs. (B) Zeta potential of DiR@PBDBM NPs.

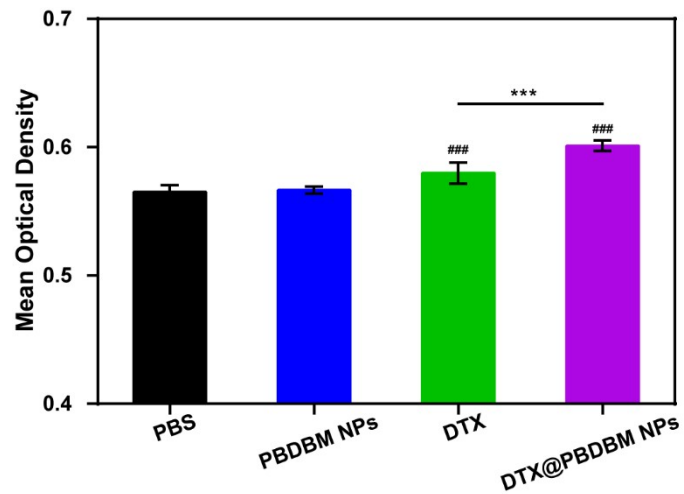


**Fig. S5.** Mean Optical Density of apoptosis calculated from TUNEL images of tumor sections after systemic administration with PBS, PBDBM NPs, DTX, and DTX@PBDBM NPs. Data were expressed as mean  $\pm$  S.D. (n = 5). \*\*\*p < 0.001 vs. DTX group; ###p < 0.001 vs. PBS group.

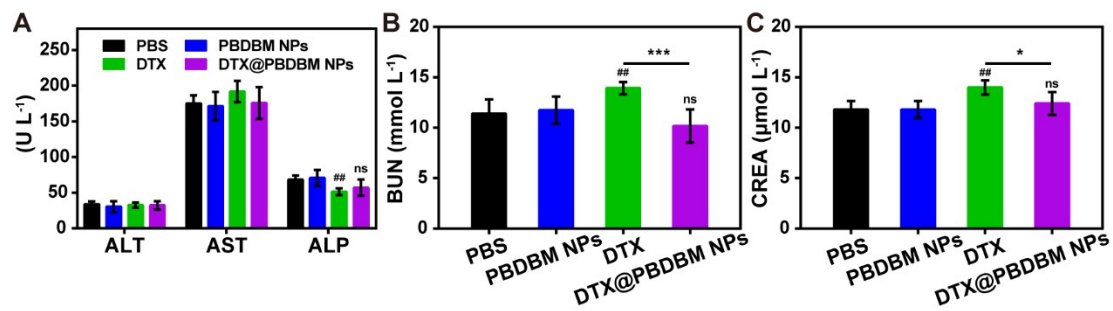


**Fig. S6.** Blood biochemical analysis of different treatments. (A) ALT, AST, ALP, (B) BUN, (C) CREA level in serum collected from 4T1 tumor-bearing mice after different treatments (n = 5, \*p < 0.05, \*\*\*p < 0.001 vs. DTX group; ##p < 0.01 vs. PBS group).



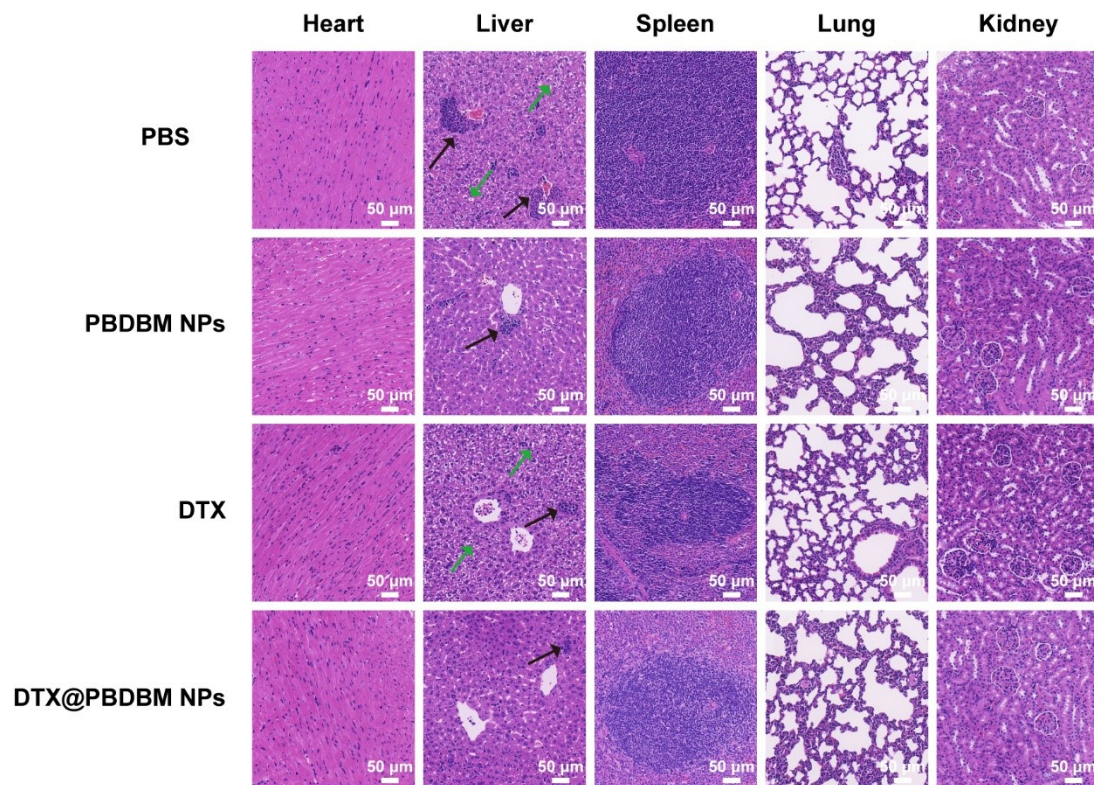


**Fig. S7.** H&E images of the major organs post systemic treatment with PBS, PBDBM NPs, free DTX, and DTX@PBDBM NPs. Magnification factor: 20×. Scale bar: 50 μm. The black arrows indicate metastatic tumors. The green arrows indicate vacuolar degeneration.